Integrative Biology

Accepted Manuscript

ROYAL SOCIETY OF CHEMISTRY

www.rsc.org/ibiology

INSIGHT STATEMENT

The work presented here provides ***Biological Insight*** by demonstrating that C-peptide, the 31-amino acid that is co-secreted in equimolar amounts with insulin in pancreatic β-cells, demonstrates specific binding to erythrocytes when carried by albumin. Efficacy was confirmed with the ***Technological Innovation*** of using a 3D-printed fluidic device with membrane inserts that enabled communication between rat INS-1 cells and an endothelium when secreted molecular messengers were delivered between the two tissues using a stream of blood components. This *in vitro* ***Integration*** of *in vivo* events was necessary to prove that albumin is required to initiate the inter-tissue communication by carrying C-peptide, and zinc, to the erythrocyte membrane.

C-peptide and Zinc Delivery to Erythrocytes Requires the Presence of Albumin: Implications in Diabetes Explored with a 3D-printed Fluidic Device

Yueli Liu, Chengpeng Chen, Suzanne Summers, Wathsala Medawala, and Dana M. Spence

Department of Chemistry
Michigan State University
East Lansing, MI, 48824
dspence@chemistry.msu.edu
517.355.9715x174

ABSTRACT

People with type 1 diabetes (T1D) must administer insulin exogenously due to the destruction of their pancreatic β-cells. Endogenous insulin is stored in β-cell granules along with C-peptide, a 31 amino acid peptide that is secreted from these granules in amounts equal to insulin. Exogenous co-administration of C-peptide with insulin has proven to reduce diabetes-associated complications in animals and humans. The exact mechanism of C-peptide's beneficial effects after secretion from the β-cell granules is not completely understood, thus hindering its development as an exogenously administered hormone. Monitoring tissue-to-tissue communication using a 3D-printed microfluidic device revealed that zinc and C-peptide are being delivered to erythrocytes by albumin. Upon delivery, erythrocyte-derived ATP increased by >50%, as did endothelium-derived NO, which was measured downstream in the 3D-printed device. Our results suggest that hormone replacement therapy in diabetes may be improved by exogenous administration of a C-peptide ensemble that includes zinc and albumin.

Diabetes now affects approximately 25.8 million people in the United States,[1] and 347 million people worldwide.[2] Currently, the core therapy for diabetes is glucose control by injecting insulin, administration of drugs, or a combination of the two.[3] Such therapies have proven effective and significantly prolong the lifespan of people with diabetes, although chronic complications often develop.[4] This is especially true for those with type 1 diabetes (T1D) where β-cell destruction in the pancreas results in essentially no insulin production.

While a single and direct cause of chronic diabetic complications remains elusive, many reports suggest that an interface dysfunction between the blood stream and peripheral tissues, resulting in vessel dysfunction, may be a major determinant.[5] For example, Low *et al.* suggested that poor blood flow results in endoneurial hypoxia, decreasing nerve signaling, resulting in neuropathy.[6] In the retina of diabetic patients, blood vessels are damaged and oxygen supply is impaired, which causes retinal cells to form new, but fragile, vessels via a vascular endothelial growth factor mechanism.[7] The breaking of the new, weak vessels can cloud the vitreous, while high vessel density is also known to be problematic. In diabetic nephropathy, the glomerulus undergoes partial sclerosis or failure to dilate, resulting in hyper filtration and subsequent protein leakage.[8] Collectively, it is anticipated that improvements in blood flow would facilitate a reduction in complications associated with diabetes. It is also likely that insulin alone is incapable of ameliorating these complications, and other therapies may be lacking.

In addition to insulin, pancreatic β-cell granules in the islets of Langerhans also produce and secrete C-peptide in equimolar amounts with insulin.[9] Since its discovery, C-peptide has long been considered a byproduct of the insulin production process without biological effects, other than facilitating the proper folding of insulin. Indeed, during the insulin production process in the β-cell granules, insulin and C-peptide are connected by disulfide bonds and constitute the proinsulin hormone.[10] Prior to secretion from the β-cell granules into the bloodstream, C-peptide is cleaved from insulin. While there are many known roles for insulin after secretion, the most-well known being the stimulation of the GLUT4 glucose transporter in fat and muscle tissue, C-peptide has often been thought to be cleared through the urine after a 30 minute half-life and without biological consequence.

Importantly, there has been increasing evidence showing that C-peptide exerts some bioactivity after release from the pancreatic β-cell granules.[11] In relation to diabetic complications, residual β-cell activity after onset of the disease had less severe complications in comparison with patients without such activity, though they received the same glucose control treatment.[12] The effects of short-term replacement of C-peptide have had beneficial effects on renal function,[13,14] blood flow,[15] and neuropathies.[16] In support of reports showing improved blood flow, our group[17] and others[18] have

shown that C-peptide enhances the ability of erythrocytes (ERYs) to release ATP, a recognized stimulus of the vessel dilator nitric oxide (NO) in the bloodstream. However, in contrast to every report showing beneficial effects of C-peptide, we have never measured any cellular effects of C-peptide unless the peptide is co-administered to the ERYs with a metal, such as Zn^{2+}.[17, 19] Unfortunately, using a variety of methods, we have never been able to demonstrate any significant binding between C-peptide and Zn^{2+} alone. Here, we report that C-peptide and Zn^{2+} delivery to the ERY requires the presence of albumin.

To confirm the necessity of each component in stimulating cellular mechanistic pathways, an *in vitro* system based on microfluidic technologies is employed. Microfluidic technologies have been used for cellular assays[20] and cell-cell communication studies[21] for over a decade and the potential for organ-on-chip and human-on-chip systems remain high.[22] A novel aspect of results reported here is the use of a 3D-printed device[23] to examine tissue-tissue communication between rat INS-1 cells (which can serve as a β-cell mimic) and an endothelium. Furthermore, key to this dynamic, *in vitro* platform is that the cellular communication between the INS-1 cells and the endothelium is carried by a stream of ERYs. Thus, this 3D-printed platform enables a complex physiological process to be investigated in a controlled manner, where systematic inhibition of certain signaling events can be performed to better understand cellular mechanistic pathways.

RESULTS

C-peptide and Zn^{2+} uptake by ERYs

Initially, we hypothesized that Zn^{2+} was facilitating delivery of C-peptide to the ERY; to investigate this hypothesis, samples of human ERYs were prepared in a physiological salt solution (PSS) in the absence and presence of C-peptide and Zn^{2+} as depicted in Fig. 1a. An ELISA for C-peptide was then used to determine the amount of C-peptide binding to the ERY in the presence and absence of Zn^{2+}. Contrary to our initial hypothesis, the data in Fig. 1b show that C-peptide binds to the ERY regardless of the presence or absence of Zn^{2+}. The C-peptide binding appears to be specific and saturates at approximately 2 picomoles, or 1800 molecules per cell in both cases. While C-peptide binds to the ERY in the presence or absence of Zn^{2+}, Fig. 1c shows that $^{65}Zn^{2+}$ uptake by ERYs occurs in the presence of C-peptide. The saturation value is statistically equal to that of C-peptide. Importantly, in the absence of C-peptide, Zn^{2+} binding to the ERYs could not be detected, suggesting that Zn^{2+} delivery to the ERY requires the presence of C-peptide.

Albumin binding to C-peptide and Zn^{2+}

The data in Figs. 2a,b, which were obtained using isothermal titration calorimetry (ITC), do not show any specific binding between C-peptide and Zn^{2+}, but rather only weak signals, regardless of the titrant, perhaps resulting from electrostatic attraction between the Zn^{2+} ions and the C-peptide's carboxylic acid-containing groups. ITC was also performed by titrating a solution of C-peptide into a solution containing human serum albumin (HSA) (Fig. 2c). The binding isotherm was fit using a one-site independent binding model where an affinity of 1.75 ± 0.64 x 10^5 M^{-1} and a binding stoichiometry of 0.53 ± 0.03 were determined, which indicates two C-peptide molecules bind to a single HSA molecule. An evaluation of HSA binding to a mixture containing both C-peptide and Zn^{2+} confirmed that HSA is able to bind both C-peptide and Zn^{2+}. The binding event between HSA and a mixture of C-peptide and Zn^{2+} was detected at pH of 7.40 (to mimic bloodstream conditions) using ITC. In Fig. 2d, a two-phase binding event occurred that could be fit into a two-site binding model with binding constants of 5.08 ± 0.98 x 10^7 M^{-1} (for Zn^{2+}) and 2.66 ± 0.25 x 10^5 M^{-1} (for C-peptide), respectively.

Enhanced ATP release from ERYs after albumin delivery of C-peptide/Zn^{2+}

ERYs from healthy donors were used to determine if albumin was required for the increase of ERY-derived ATP in the presence of C-peptide and Zn^{2+}. Samples were prepared (Fig. 3a) in a manner similar to that shown in Fig. 1a; specifically, in the presence and/or absence of C-peptide and Zn^{2+}. However, these combinations were also prepared with and without HSA. These samples were then pumped through a 3D-printed microfluidic device that contained a 6 mm transwell insert. The insert bottom is comprised of a membrane with 0.4 micron pores that allow ATP to pass from the channel of the device to the area above the membrane where it is mixed with a solution of luciferin and luciferase to generate a chemiluminescent signal proportional to the amount of ATP released from the ERYs. ERYs incubated with C-peptide and Zn^{2+} in PSS stimulated the highest ATP release (319.8 ± 15.2 nM), which was significantly higher than the ERYs in the absence of C-peptide/Zn^{2+} in PSS as a control group (194.9 ± 19.7 nM, $p < 0.005$). ERYs incubated with C-peptide or Zn^{2+} alone, whether in the presence of HSA or not, did not show significant ATP release increase. When the same ERY samples were incubated in albumin-free PSS, significant increases in ATP release could not be detected (216.9 ± 23.3 nM vs. 206.8 ± 19.4 nM), even in the presence of C-peptide/Zn^{2+}.

A 3D-printed fluidic device reveals possible overlooked importance of C-peptide in type I diabetes

Fig. 4a shows the top-down view of the strategy employed to verify downstream effects of the INS-1 secretions, while Fig. 4b is a side-view of the system, showing ERYs circulating underneath the various inserts. Once a 7% solution of ERYs (in PSS) was circulating through the system, the INS-1 cells (located in the top insert, represented by the blue ovals) were stimulated with a 12 mM solution of glucose. The secretions from these cells, which include C-peptide and Zn^{2+}, diffuse through the membrane and into the channel where they are carried to the ERYs. ERYs were pumped through the channels in PSS, except for channel 2, which was albumin-free PSS. After 20 minutes of circulating the ERYs through the system, measurements of ATP in the middle inserts (orange circles) and NO in the bottom inserts (green circles) were performed by placing the fluidic device in a plate reader. The data in Fig. 4c clearly show ATP levels are only increased when INS-1 cells are stimulated with glucose and albumin is present in the flowing stream of ERYs (channel 1). It is anticipated that this increase in ATP release from the ERYs is due to the release of C-peptide and Zn^{2+} from the INS-1 cells, which is subsequently carried to the ERYs by albumin in the PSS. Note in Fig. 4c that the absence of albumin in the stream of ERYs (channel 2) results in no significant increase in ATP release. There is also no increase in ATP release in the absence of INS-1 cells in the first well (clear oval in channel 3). In channel 4, the system contained INS-1 cells and albumin while the third well containing endothelial cells was incubated with PPADs, a P2Y purinergic receptor inhibitor. This antagonist was added to block ATP binding to the endothelial cells for inhibition of NO production; therefore, it has no effect on ATP release. Fig. 4d shows similar trends for measurement of ERY-derived ATP, although these measurements represent the amount of ATP determined in the channels underlying the membrane-based inserts.

Fig. 4e contains results from measurements of NO from the bottom wells on each channel. These wells contained endothelial cells which, upon stimulation with ATP, will produce NO. As expected, based on data in Fig. 4c, the most NO production is measured when glucose is used to stimulate INS-1 cells in the presence of an albumin-containing buffered stream of ERYs (channel 1). In the absence of albumin (channel 2), there is reduced ATP release, thus resulting in decreased amounts of NO being produced. Reduced levels of NO were also measured when there were no INS-1 cells in the first well (channel 3); again, reduced ATP in channel 3 (both insert and channel) suggests that reduced levels of NO would be measured this channel, and this is confirmed in Fig. 4e. Finally, the last bar in Fig. 4e shows that the addition of the ATP receptor blocker, PPADS, blocks ATP released by the ERY from binding to the endothelial cells, thus inhibiting NO production.

DISCUSSION

C-peptide, the 31 amino acid peptide that is co-secreted in equimolar amounts with insulin from pancreatic β-cell granules, has been shown to display beneficial health effects in animals and humans with type 1 diabetes (T1D).[11, 24] Improved outcomes related to such diabetic complications as neuropathy and nephropathy have been reported,[16] as are improvements in blood flow in skin and muscle tissue.[15, 25] Recently, it has been shown to reduce post-hemorrhagic shock in male rats.[26] Despite these and other reports demonstrating biological efficacy of C-peptide, C-peptide's use as a replacement therapy for people with T1D (who no longer produce insulin or C-peptide) has been slow to develop for a multitude of reasons, including the lack of an identified receptor for C-peptide.[27]

In previous studies performed by our group involving C-peptide and its effects on ERYs, ATP release from ERYs could only be elicited when these cells were added to a buffer containing C-peptide and a transition metal ion.[17] The metal that was originally discovered to play a role in C-peptide/metal activity was iron (Fe^{2+}), which was determined by mass spectrometry to be an impurity in the commercially obtained C-peptide. Due to its well-established presence at millimolar levels in the pancreatic β-cell granules (where C-peptide and insulin are also stored prior to secretion), we suspected that Zn^{2+} may be the metal responsible for cellular activity *in vivo*. A subsequent report confirmed that Zn^{2+}, in the presence of C-peptide, is able to stimulate ATP release from ERYs.[19] The addition of either C-peptide or Zn^{2+} alone did not result in an increase in ERY-derived ATP, resulting in the initial hypothesis that Zn^{2+} may somehow facilitate delivery of C-peptide to the ERY. Results in Fig. 1 prove our initial hypothesis concerning the role of Zn^{2+} incorrect, as our data show that C-peptide binds to the ERYs in the presence or absence of Zn^{2+}, but that Zn^{2+} delivery to the ERY required the presence of C-peptide. While our initial hypothesis was incorrect, the notion of C-peptide binding to cells in the absence of exogenously added is metal is not without precedence. Despite the lack of a receptor, C-peptide displays specific binding to such cells as human renal tubular cells, fibroblasts, and venous endothelial cells.[28] Here, we report similar binding characteristics of C-peptide to human ERYs.

Despite our data suggesting that Zn^{2+} delivery to the ERY required, numerous attempts to demonstrate C-peptide binding to Zn^{2+} were unsuccessful. Due to the absence of binding between C-peptide and Zn^{2+}, it was anticipated that another molecule in our system was participating in the delivery of Zn^{2+} to the ERY. The PSS used in all previous studies by our group involving C-peptide contained albumin, a protein well known for its ability to serve as a carrier of peptides, proteins, and drug molecules *in vivo*.[29] Here, we noticed that solubility of C-peptide in PSS is enhanced when albumin is present, although we do not suspect this enhanced solubility as the sole reason behind C-peptide

binding to the ERY as the C-peptide is soluble in solution even in the absence of albumin. The binding data in Fig. 2c suggests that albumin is a determinant in C-peptide and Zn^{2+} binding and perhaps delivery to the ERY, thus prompting a reappraisal of the ELISA-based measurements of C-peptide binding to the ERYs, as well as the radioisotopic determination of Zn^{2+} delivery to the ERYs (shown in Figs. 1b and 1c). As anticipated, C-peptide binding to the ERY could not be detected in the absence of albumin; furthermore, Zn^{2+} delivery to the ERY was also absent in an albumin-free version of PSS, regardless if C-peptide was present (data not shown). These results show that the presence of albumin is necessary for C-peptide and Zn^{2+} delivery to the ERY.

Although the 3-component ensemble seems to be necessary for delivery of C-peptide and Zn^{2+} to the ERY, a structure of this system is not yet known, nor are the binding sites completely understood. In the literature, it is well-established that the glutamic acid residue at position 27 (E27) is required for C-peptide to affect cells.[11, 30] Interestingly, many linkages between albumin molecules and other peptides and proteins often occur through carboxylate linkages. Here, an E27 mutant to alanine (E27A) was prepared and its ability to bind albumin using ITC was determined to be essentially non-existent, as shown in Supplementary Fig. S1a. Furthermore, using radioisotopic assays, it was determined that the mutant (when used in the 3-component ensemble with albumin and Zn^{2+}) could not successfully deliver Zn^{2+} to the ERY (Fig S1b). The binding of the mutant itself to the ERY was not determined as the ELISA kit (using an antibody for C-peptide) could not detect the mutant. Collectively, the data shown here may explain past reports that emphasize the importance of E27; without E27 present in C-peptide, binding to albumin is reduced and therefore the peptide is not delivered to the cell. These results are of particular importance considering that, in the studies reported here, rat C-peptide was used in conjunction with human ERYs. Rat C-peptide and human C-peptide have dissimilar sequences. However, the glutamic acid at position 27 is conserved in both species; in this construct, based on past results showing the importance of E27 in C-peptide, it is probable that C-peptide from different species (having different sequences) may still show activity on cells derived from different species.

While the data in Figs. 1 and 2 suggest that albumin is required for C-peptide and Zn^{2+} delivery to the ERY, such static measurements do not provide any information about the potential mechanism by which C-peptide improves blood flow in both animal and human T1D subjects. A 3D-printed fluidic device was designed and fabricated that enables dynamic and flow-based investigations of ERYs with C-peptide, Zn^{2+}, and albumin. The results summarized in Fig. 3, showing an increase in ATP release from ERYs incubated with C-peptide/Zn^{2+}/albumin, support the results from our binding studies.

In order to create a more realistic version of *in vivo* events using our 3D-printed *in vitro* platform, rat INS-1 cells, which are capable of secreting both insulin and C-peptide and contain the ZnT-8 protein (a protein found in β–cell granules responsible for transport of Zn^{2+}), were cultured on 6 mm transwell membrane inserts placed in the fluidic device. Upon INS-1 stimulation with glucose, ATP release and subsequent NO production by endothelial cells could only be detected when the INS-1 cells and ERYs were present and when the ERYs were in a buffered stream that contained albumin. Importantly, the data shown in Supplementary Fig. S3a,b show the C-peptide secretion levels in the insert over a time course of about 2 hours and the concentration of C-peptide that was able to diffuse into the device channels and affect the flowing stream of ERYs is shown in Supplementary Fig. S3c,d. These concentrations, between 0.5 nM and 2.0 nM, are similar to those reported to occur *in vivo*. Therefore, not only do the results here involve complete characterization and validation of C-peptide purity using mass spectrometry prior to use, we also validate the concentration affecting the cells in this study.

The downstream, pathophysiological importance of the C-peptide/ Zn^{2+}/albumin effects is shown by the measurement of the important vasodilator, NO. The use of PPADs, a known inhibitor of the ATP binding site on endothelial cells, reduced endothelium-derived NO production, confirming that the increase in measured NO was due to ATP release which, in turn, had been stimulated by albumin delivery of C-peptide/Zn^{2+} to the flowing ERYs.

While the data presented here strongly suggests a role for albumin in the delivery of C-peptide and Zn^{2+} to the ERY, it should be noted that the necessity of Zn^{2+} in conjunction with C-peptide is not without precedence. Multiple reports have shown that the addition of EDTA to various C-peptide formulations abolished all cellular/tissue effects.[31] It was suspected that the added EDTA was binding to Ca^{2+} stores necessary for cellular function. However, based on relative binding affinities of EDTA to Zn^{2+} and Ca^{2+}, it is much more likely that EDTA was competitively binding Zn^{2+} prior to delivery to cells *in vivo*. Separate studies have shown that Zn^{2+} supplementation prior to addition of C-peptide in hemorrhagic shock reduced inflammatory pathways when compared to addition of C-peptide alone.[32]

CONCLUSION

Since its discovery nearly 50 years ago, the biological role of C-peptide has been mostly limited to facilitating the proper folding of insulin in the β-cell granules prior to secretion into the bloodstream, despite numerous studies showing benefits outside of this role. Here, we demonstrate that C-peptide binding to ERYs requires the presence of albumin. Furthermore, binding of Zn^{2+} to the ERY, a requisite for the release of ATP from these cells, only occurs in the presence of both albumin and C-peptide. A

3D-printed fluidic device was used to demonstrate that ERYs, when flowing in an albumin-containing buffer underneath INS-1 cells, secreted significant increased amounts of ATP. Downstream effects of the increased ATP included enhanced NO production by a cultured endothelium, thus possibly explaining the improved blood flow characteristics seen in animal and human T1D subjects when administered C-peptide.

Despite our findings, enhanced *in vitro* platforms are still required in order to gain a complete understanding of the β-cell secretions from the Islets of Langerhans and their effect on cells and tissues. Studies demonstrating beneficial effects of C-peptide usually require co-administration of insulin. Indeed, synergistic effects between insulin and C-peptide exist. Specifically, Sprague has shown that ATP release from ERYs incubated with C-peptide and insulin is largely dependent upon the C-peptide: Zn^{2+} ratio in the sample.[33] The ATP release was stimulated by exposing the ERYs to a hypoxic environment after incubation in solutions with various C-peptide:insulin concentration ratios. We have previously shown that the addition of insulin to C-peptide (rather than a Zn^{2+} salt, such as $ZnCl_2$) is capable of stimulating ATP release from ERYs. In contrast, when a Zn^{2+}-free version of insulin was used, or when EDTA was co-administered with a Zn^{2+}-containing form of insulin, there was no significant increase in ATP release from the ERYs.[34] It is anticipated that preparation and characterization of C-peptide with mass spectrometry prior to use, as well as the addition of albumin and Zn^{2+} in known stoichiometry, will enhance precision and understanding of C-peptide's biological effects beyond ATP release and downstream NO production. For example, a C-peptide receptor has never been discovered. If albumin is a determinant in C-peptide binding to cells, it may accelerate attempts to find the elusive C-peptide receptor. It may also be possible to now grow crystals containing albumin, Zn^{2+}, and C-peptide to determine a structure of the assembly that may be involved in receptor-based binding.

Experimental

Collection and purification of ERYs

All procedures involving human subjects, including consent forms, were approved by the Biomedical and Health Institutional Review Board (BIRB) at Michigan State University. Whole blood was obtained from consented healthy human donors by venipuncture and collected into heparinized tubes. Blood was then centrifuged at 500 *g* for 10 min and the plasma and buffy coat were removed by aspiration. ERYs were

washed 3 times in a physiological salt solution (PSS, in mM, 4.7 KCl, 2.0 $CaCl_2$, 140.5 NaCl, 12 $MgSO_4$, 21.0 tris(hydroxymethyl) aminomethane, 5.5 glucose, and 5% bovine serum albumin, final pH = 7.40). All reagents were purchased from Sigma-Aldrich (St. Louis, MO). For all albumin free experiments, ERYs were washed in albumin-free PSS. The hematocrit was determined using a hematocrit measurement device (CritSpin, Iris sample processing, Westwood, MA).

ELISA-based determination of C-peptide binding to ERYs

C-peptide binding to ERYs in the presence and absence of albumin was performed using a commercially available ELISA kit. ERY samples (7% hematocrit) were prepared in either PSS or in albumin-free PSS. These PSS solutions, prior to the addition of the ERYs, contained varying (0, 1, 2, 4, 10, 20 nM) concentrations of C-peptide (Genscript, Piscataway, NJ). For certain studies, these solutions were also prepared to contain 0-20 nM Zn^{2+}. All samples were incubated at 37 °C for 2 hours after the addition of the ERYs. Next, samples were centrifuged at 500 *g* for 5 min and the supernatant was collected and used as the sample in the ELISA-based determination of C-peptide. This particular ELISA assay is a sandwich-based assay using an enzymatically-tagged secondary antibody that catalyzes a colorimetric reaction. The absorbance of the product of this reaction was measured using a standard plate reader at 450 nm (Molecular Devices LLC, Sunnyvale, CA). To determine the C-peptide uptake by the cells at each concentration point, the moles of C-peptide remaining in the supernatant were subtracted from the original number of moles added to the ERYs.

Radiometric determination of $^{65}Zn^{2+}$ uptake by ERYs

To determine if albumin and C-peptide are necessary for Zn^{2+} uptake by the ERY, samples containing 7% ERYs (by volume) were prepared in either PSS or albumin-free PSS, with varying concentrations (0, 1, 2, 4, 10, 20 nM) of combined C-peptide and $^{65}Zn^{2+}$, or $^{65}Zn^{2+}$ alone. All samples were incubated at 37 °C for 2 hours after the addition of the ERYs. Next, samples were centrifuged at 500 *g* for 5 min, and the supernatant was collected. The amount of $^{65}Zn^{2+}$ remaining in the supernatant was measured using a scintillation counter after mixing 200 µL of each supernatant with 100 µL of scintillation cocktail. The amount of $^{65}Zn^{2+}$ uptake by the cells at each concentration point was determined by subtracting the $^{65}Zn^{2+}$ concentration in the supernatant from the originally added concentration.

Isothermal titration calorimetry (ITC)

Data for determination of all thermodynamic parameters were obtained using a microisothermal titration calorimeter (ITC) (MicroCal, Piscataway, NJ) at 25 °C. All solutions used for ITC experiments were prepared in 0.5 mM Tris-HCl buffer at a pH of 7.40 ± 0.01, except for C-peptide/Zn^{2+} titrations, which were prepared in doubly deionized water (DDW, 18.2 MΩ). Before ITC titration, commercially available C-peptide was further purified by HPLC and confirmed by mass spectrometry. Determination of the enthalpy of reaction requires known concentrations; therefore, the concentration of purified human C-peptide solution was determined by human C-peptide ELISA, and the concentration of human serum albumin (HSA) solution by Pierce BCA Protein Assay Kit (Thermo Scientific, Rockford, IL).

All ITC experiments were performed using 10 µL titrant injections into a 1 mL volume in an adiabatic cell, 120 s spacing between injections, and 310 rpm stirring speed. ITC measurements of C-peptide interactions with Zn^{2+} were performed by titration of a 3 mM Zn^{2+} solution into a 250 µM C-peptide solution, or by titrating a 250 µM C-peptide solution into a 20 µM Zn^{2+} solution. ITC measurements of C-peptide binding to HSA were performed by titration of a 225 µM HSA solution into a 30 µM C-peptide solution. Measurements of combined C-peptide and Zn^{2+} binding to HSA were performed by titration of a 225 µM HSA solution into a pre-mixed solution containing C-peptide/Zn^{2+}, each at 25 µM. Measurements of E27A (Peptide 2.0 Inc., Chantilly, VA) binding to HSA was performed by titration of a 200 µM HSA solution into a 20 µM E27A solution. The background dilution heats were determined in separate experiments by titration of HSA solution into buffer, and buffer into C-peptide, C-peptide/Zn^{2+}, and E27A solution. All measurements were performed at least in triplicate to confirm reproducibility. The net heat obtained was analyzed using the one-site independent binding model implemented by Origin software, with the exception of the HSA titration to C-peptide and Zn^{2+}, where a two-site independent binding model was used to obtain the net heat.

Measurement of ATP on a 3-D printed fluidic device

ATP was quantified by the luciferase/luciferin chemiluminescence assay (L/L assay) on a 3-D printed fluidic device previously described and characterized by our group.[35] The device design was modeled as a 96-well plate for subsequent measurement on a standard plate reader. Six channels were fabricated in the device, with wells above these channels that align with the internal robotics of the plate reader for measurement convenience. A 6 mm diameter transwell insert whose bottom is porous polyester (0.4 micron) is placed in each of the wells. During use, ERY samples flow through the channels and released ATP is able to diffuse through the membrane pores into buffer that was pre-loaded in the

insert above the membrane. Aliquots (10 μL) of the L/L mixture were then injected into each well, and the entire device was placed in the plate reader for chemiluminescence measurement.

Before measuring ERY samples, a calibration curve was obtained by circulating four ATP standards prepared in PSS (concentrations of 0, 100, 200 and 400 nM) in four randomly chosen channels at a flow rate of 50 μL/min using a peristaltic pump (IDEX Health & Science LLC, Oak Harbor, WA) as part of the pumping mechanism. To facilitate ATP diffusion through the membrane pores and into the well insert, 50 μL of PSS was loaded in the membrane inserts on row E above each channel. After flowing for 20 minutes, the 3D-printed device was detached from the peristaltic pump tubing and was placed on the holder of a plate reader (Molecular Devices LLC, Sunnyvale, CA), followed by the simultaneous addition of 10 μL of L/L assay mixture into each insert to measure chemiluminescence intensity values resulting from the reaction of the L/L mixture with ATP. A standard curve was generated by plotting the chemiluminescence intensity values against the known concentrations of ATP.

Four samples were prepared containing ERYs at a 7% hematocrit in different conditions: buffer only, buffer with C-peptide, buffer with both C-peptide and Zn^{2+} ($ZnCl_2$), and buffer with Zn^{2+}. Buffer choices included PSS and albumin-free PSS in order to study the effect of albumin on C-peptide and Zn^{2+} delivery to the ERYs, as well as subsequent ATP release from the ERYs. C-peptide and Zn^{2+} stock solutions (800 nM for both) were prepared in doubly deionized water (DDW, 18.2 MΩ). The working samples (10 nM) were then pumped to fill four randomly chosen channels on the device, after which each channel and corresponding tubing were closed to form a loop. The samples with different C-peptide treatments were then introduced into the device to form four circulating loops. The whole setup was then placed in a 37 °C incubator for 2 hours, during which, C-peptide/Zn^{2+}/albumin that were mixed in circulating ERY samples would exert their effect on the cells. The entire set up of pump, device, and closed loops with circulating samples were placed in an incubator at 37 °C. The samples were allowed to circulate through the system for 1.5 h. 50 μL of PSS were loaded in the inserts in row E to collect ATP from samples via diffusion through the pores in the insert membrane. ERY-derived ATP was determined in the same manner as the ATP standards, other than the fact that a stream of ERYs was delivered through the channels as opposed to ATP standards.

Cell to cell communication using a 3D-printed fluidic platform

The membrane inserts were prepared for cell culture by coating the membrane with 30 μL of a fibronectin solution (50 μg/mL), and subsequent sterilization by exposure to UV light. Rat INS-1 cells

were cultured in RPMI-1640 medium (Life technologies, Carlsbad, CA) with 1 mM sodium pyruvate, 100 U/mL penicillin, 100 µg/mL streptomycin, 55 µM mercaptoethanol, 10% fetal bovine serum, 2 mM L-glutamine and 10 mM HEPES. When the cells were confluent, as verified by optical microscopy, they were detached from the flask with trypsin/EDTA, then centrifuged at 1000 *g* for 4 min. The pellet was resuspended in 400 µL of the RPMI-1640 medium. Cell density was by hemacytometer (Reichert, Buffalo, NY), based on which, the cell suspension was further diluted to a cell density of 0.1 million/µL. An aliquot of 200 µL of the cell suspension was added into a coated membrane insert, which was then placed in an incubator with 5% CO_2 at 37 °C. After two hours, the medium in the inserts was removed and 200 µL fresh medium was added. The cells were given another 24 hours incubation to grow before using on the 3D printed fluidic platform. Prior to use, the medium was removed and 200 µL Krebs buffer containing 12 mM glucose and 0.1 % albumin was added to stimulate secretion of these cells for 1 hour.

Endothelial cell culture was accomplished using bovine pulmonary arterial endothelial cells (bPAECs) that were cultured in T-75 flasks with DMEM media containing 5.5 mM glucose, 10% (v/v) fetal bovine serum, and penicillin/streptomyocin. When the cells were confluent as verified with optical microscopy, they were detached from the flask with trypsin/EDTA and centrifuged at 1500 *g* for 5 min. The pellet was then resuspended in 400 µL of the DMEM media. Cell density was determined by hemacytometer, and the cell suspension was then diluted to a density of 0.05 million/µL. An aliquot of 200 µL of the cell suspension was added into a coated membrane insert, which was then placed in an incubator with 5% CO_2 at 37 °C. After two hours, the medium in the inserts was removed and 200 µL of fresh medium were added. The cells were given another 24 hours to grow before using on the 3D printed fluidic device. PPADS (pyridoxalphosphate-6-azophenyl-2', 4'-disulfonic acid) was used in the experiments involving inhibition of P2Y receptors on endothelial cells. A PPADS working solution was prepared by diluting 50 µL of 100 mM PPADS stock solution (in DMSO) with 450 µL of Hanks' balanced salt solution (HBSS) to create a final concentration of 10 mM. DMEM medium was removed from the insert, followed by rinsing with HBSS. Next, 50 µL of the PPADS working solution was added to the insert. After a 30 min incubation at 37 °C, the insert was rinsed with HBSS to remove excess PPADS solution.

Images of the circulation platform setup can be found in Fig. S2. The same 3D printed device used to quantify ATP was used here to set up a 3-tissue, circulation mimic platform. When β-cells and endothelial cells cultured in membrane inserts were ready to use, the insert with β-cells was placed into well #1, while the endothelial cell insert was placed into well #3. The bPAEC medium was then removed and replaced by 200 µL of HBSS. A clean insert was placed in well #2 for ATP collection. As mentioned

above, fresh ERYs at a 7% hematocrit were prepared in corresponding buffers (albumin-containing or albumin-free PSS), and then pumped into each channel to form a closed-loop circulation. The entire setup was then placed in a 37 °C incubator. The peristaltic pump was then started, and ERYs circulated at 200 µL/min in the loop (circulation period was around 2 min) for 2 hours.

ERY-derived ATP was quantified in well #2 as detailed above. A fluorescent probe DAF (4-amino-5-methylamino, Invitrogen Inc.) was used for the quantitative determination of endothelium-derived NO. To prepare working solutions, 1 mg of DAF was dissolved in DMSO to make a 5 mM solution. This solution was diluted to 25 µM in HBSS immediately before use. An aliquot of 50 µL of this DAF solution was then added into the endothelial cell inserts, to react with produced NO. After circulation of the ERYs for 2 hours, the detached bulk device was placed in the plate reader for fluorescence detection (ex 480 nm, em 520 nm) above corresponding wells to quantify NO. The NO donor Spermine NONOate (Cayman Chemicals, Ann Arbor, MI), whose half-life is 37 min, was applied in this study to prepare standard NO solutions for calibration. Spermine NONOate was dissolved in 0.01 M NaOH as a 1 mM stock solution, which can be stored at -20 °C for several months. This stock solution was diluted in HBSS to four standard solutions of 0, 0.5, 1, and 2 µM, followed by immediate addition of 25 µM DAF solution (100 µL of DAF solution into 400 µL of Spermine NONOate solution). The mixed solutions were then kept in the dark (to reduce photobleaching) and placed in a 37 °C incubator for 40 min, after which, 250 µL of each mixed solution were pipetted into the four inserts on column 10 of the fluidic device, which was then placed in the plate reader for fluorescence intensity measurement. A calibration curve was obtained by plotting fluorescence intensity versus the corresponding NO concentration.

Statistical analysis

Analysis of means was performed using a paired t-test. p-values showing the level of statistical significance associated with certain figures are provided in the figures and in the text.

References:

1. Fast Facts: Data and Statistics about Diabetes. *American Diabetes Association* 2013.
2. G. Danaei, M. M. Finucane, Y. Lu, G. M. Singh, M. J. Cowan, C. J. Paciorek, J. K. Lin, F. Farzadfar, Y. H. Khang, G. A. Stevens, M. Rao, M. K. Ali, L. M. Riley, C. A. Robinson, M. Ezzati, G. B. M. R. F. C, National, regional, and global trends in fasting plasma glucose and diabetes prevalence since 1980: systematic analysis of health examination surveys and epidemiological studies with 370 country-years and 2.7 million participants. *Lancet* 2011, *378*. 31-40, DOI: Doi 10.1016/S0140-6736(11)60679-X.
3. H. Yki-Jarvinen, Combination therapies with insulin in type 2 diabetes. *Diabetes Care* 2001, *24*. 758-767, DOI: DOI 10.2337/diacare.24.4.758.
4. M. J. Fowler, Microvascular and Macrovascular Complications of Diabetes. *Clinical Diabetes* 2008, *26*. 77-82.
5. (a) G. E. Mcveigh, G. M. Brennan, G. D. Johnston, B. J. Mcdermott, L. T. Mcgrath, W. R. Henry, J. W. Andrews, J. R. Hayes, Impaired Endothelium-Dependent and Independent Vasodilation in Patients with Type-2 (Non-Insulin-Dependent) Diabetes-Mellitus. *Diabetologia* 1992, *35*. 771-776; (b) S. B. Williams, J. A. Cusco, M. A. Roddy, M. T. Johnstone, M. A. Creager, Impaired nitric oxide-mediated vasodilation in patients with non-insulin-dependent diabetes mellitus. *Journal of the American College of Cardiology* 1996, *27*. 567-574, DOI: Doi 10.1016/0735-1097(95)00522-6.
6. P. A. Low, J. D. Schmelzer, K. K. Ward, G. L. Curran, J. F. Poduslo, Effect of Hyperbaric Oxygenation on Normal and Chronic Streptozotocin Diabetic Peripheral-Nerves. *Experimental Neurology* 1988, *99*. 201-212, DOI: Doi 10.1016/0014-4886(88)90139-2.
7. E. A. Pierce, R. L. Avery, E. D. Foley, L. P. Aiello, L. E. H. Smith, Vascular Endothelial Growth-Factor Vascular-Permeability Factor Expression in a Mouse Model of Retinal Neovascularization. *Proceedings of the National Academy of Sciences of the United States of America* 1995, *92*. 905-909, DOI: DOI 10.1073/pnas.92.3.905.
8. P. A. Craven, M. A. Caines, F. R. Derubertis, Sequential Alterations in Glomerular Prostaglandin and Thromboxane Synthesis in Diabetic Rats - Relationship to the Hyperfiltration of Early Diabetes. *Metabolism-Clinical and Experimental* 1987, *36*. 95-103, DOI: Doi 10.1016/0026-0495(87)90070-9.
9. A. H. Rubenstein, J. L. Clark, F. Malani, D. F. Steiner, Secretion of Proinsulin C-Peptide by Pancreatic Beta Cells and Its Circulation in Blood. *Nature* 1969, *224*. 697-&, DOI: Doi 10.1038/224697a0.
10. D. F. Steiner, Role of Proinsulin C-Peptide. *Diabetes* 1978, *27*. 145-148.
11. J. Wahren, K. Ekberg, H. Jornvall, C-peptide is a bioactive peptide. *Diabetologia* 2007, *50*. 503-509, DOI: DOI 10.1007/s00125-006-0559-y.
12. S. Sjoberg, M. Gjotterberg, L. Berglund, E. Moller, J. Ostman, Residual C-peptide excretion is associated with a better long-term glycemic control and slower progress of retinopathy in type I (insulin-dependent) diabetes mellitus. *J Diabet Complications* 1991, *5*. 18-22.
13. B. L. Johansson, S. Sjoberg, J. Wahren, The Influence of Human C-Peptide on Renal-Function and Glucose-Utilization in Type-1 (Insulin-Dependent) Diabetic-Patients. *Diabetologia* 1992, *35*. 121-128, DOI: Doi 10.1007/Bf00402543.
14. B. L. Johansson, A. Kernell, S. Sjoberg, J. Wahren, Influence of combined C-peptide and insulin administration on renal function and metabolic control in diabetes type 1. *J Clin Endocrinol Metab* 1993, *77*. 976-81, DOI: 10.1210/jcem.77.4.8408474.
15. T. Forst, T. Kunt, Effects of C-peptide on microvascular blood flow and blood hemorheology. *Experimental Diabesity Research* 2004, *5*. 51-64, DOI: Doi 10.1080/15438600490424532.
16. (a) B. L. Johansson, K. Borg, E. Fernqvist-Forbes, A. Kernell, T. Odergren, J. Wahren, Beneficial effects of C-peptide on incipient nephropathy and neuropathy in patients with Type 1 diabetes mellitus.

Diabetic Med 2000, *17*. 181-189, DOI: DOI 10.1046/j.1464-5491.2000.00274.x; (b) A. A. F. Sima, H. Kamiya, Is C-peptide replacement the missing link for successful treatment of neurological complications in type 1 diabetes? *Current Drug Targets* 2008, *9*. 37-46, DOI: Doi 10.2174/138945008783431745.

17. J. A. Meyer, J. M. Froelich, G. E. Reid, W. K. Karunarathne, D. M. Spence, Metal-activated C-peptide facilitates glucose clearance and the release of a nitric oxide stimulus via the GLUT1 transporter. *Diabetologia* 2008, *51*. 175-82, DOI: 10.1007/s00125-007-0853-3.
18. J. P. Richards, A. H. Stephenson, M. L. Ellsworth, R. S. Sprague, Synergistic effects of C-peptide and insulin on low O-2-induced ATP release from human erythrocytes. *Am J Physiol-Reg I* 2013, *305*. R1331-R1336, DOI: DOI 10.1152/ajpregu.00341.2013.
19. J. A. Meyer, W. Subasinghe, A. A. F. Sima, Z. Keltner, G. E. Reid, D. Daleke, D. M. Spence, Zinc-activated C-peptide resistance to the type 2 diabetic erythrocyte is associated with hyperglycemia-induced phosphatidylserine externalization and reversed by metformin. *Molecular Biosystems* 2009, *5*. 1157-1162, DOI: Doi 10.1039/B908241g.
20. (a) S. Takayama, E. Ostuni, P. LeDuc, K. Naruse, D. E. Ingber, G. M. Whitesides, Selective chemical treatment of cellular microdomains using multiple laminar streams. *Chem Biol* 2003, *10*. 123-130, DOI: Doi 10.1016/S1074-5521(03)00019-X; (b) R. S. Kane, S. Takayama, E. Ostuni, D. E. Ingber, G. M. Whitesides, Patterning proteins and cells using soft lithography. *Biomaterials* 1999, *20*. 2363-2376, DOI: Doi 10.1016/S0142-9612(99)00165-9.
21. (a) L. I. Genes, N. V. Tolan, M. K. Hulvey, R. S. Martin, D. M. Spence, Addressing a vascular endothelium array with blood components using underlying microfluidic channels. *Lab Chip* 2007, *7*. 1256-1259, DOI: Doi 10.1039/B712619k; (b) C. J. Ku, T. D. Oblak, D. M. Spence, Interactions between multiple cell types in parallel microfluidic channels: Monitoring platelet adhesion to an endothelium in the presence of an anti-adhesion drug. *Anal Chem* 2008, *80*. 7543-7548, DOI: Doi 10.1021/Ac801114j.
22. D. Huh, H. J. Kim, J. P. Fraser, D. E. Shea, M. Khan, A. Bahinski, G. A. Hamilton, D. E. Ingber, Microfabrication of human organs-on-chips. *Nat Protoc* 2013, *8*. 2135-2157, DOI: DOI 10.1038/nprot.2013.137.
23. B. C. Gross, J. L. Erkal, S. Y. Lockwood, C. P. Chen, D. M. Spence, Evaluation of 3D Printing and Its Potential Impact on Biotechnology and the Chemical Sciences. *Anal Chem* 2014, *86*. 3240-3253, DOI: Doi 10.1021/Ac403397r.
24. (a) J. Wahren, A. Kallas, A. A. F. Sima, The Clinical Potential of C-Peptide Replacement in Type 1 Diabetes. *Diabetes* 2012, *61*. 761-772, DOI: Doi 10.2337/Db11-1423; (b) A. A. F. Sima, Diabetes & C-Peptide Scientific and Clinical Aspects Conclusions and Future Outlook. *Diabetes & C-Peptide: Scientific and Clinical Aspects* 2012. 161-163, DOI: Doi 10.1007/978-1-61779-391-2_14.
25. T. Forst, D. D. De la Tour, T. Kunt, A. Pfutzner, K. Goitom, T. Pohlmann, S. Schneider, B. L. Johansson, J. Wahren, M. Lobig, M. Engelbach, J. Beyer, P. Vague, Effects of proinsulin C-peptide on nitric oxide, microvascular blood flow and erythrocyte Na+,K+-ATPase activity in diabetes mellitus type I. *Clinical Science* 2000, *98*. 283-290, DOI: Doi 10.1042/Cs19990241.
26. R. S. Chima, G. Maltese, T. LaMontagne, G. Piraino, A. Denenberg, M. O'Connor, B. Zingarelli, C-Peptide Ameliorates Kidney Injury Following Hemorrhagic Shock. *Shock* 2011, *35*. 524-529, DOI: Doi 10.1097/Shk.0b013e31820b2e98.
27. L. Luzi, G. Zerbini, A. Caumo, C-peptide: a redundant relative of insulin? *Diabetologia* 2007, *50*. 500-2, DOI: 10.1007/s00125-006-0576-x.
28. R. Rigler, A. Pramanik, P. Jonasson, G. Kratz, O. T. Jansson, P. A. Nygren, S. Stahl, K. Ekberg, B. L. Johansson, S. Uhlen, M. Uhlen, H. Jornvall, J. Wahren, Specific binding of proinsulin C-peptide to human cell membranes. *Proceedings of the National Academy of Sciences of the United States of America* 1999, *96*. 13318-13323, DOI: DOI 10.1073/pnas.96.23.13318.

29. (a) M. E. Baker, Albumin's role in steroid hormone action and the origins of vertebrates: is albumin an essential protein? *Febs Letters* 1998, *439*. 9-12, DOI: Doi 10.1016/S0014-5793(98)01346-5; (b) F. Kratz, Albumin as a drug carrier: Design of prodrugs, drug conjugates and nanoparticles. *Journal of Controlled Release* 2008, *132*. 171-183, DOI: DOI 10.1016/j.jconrel.2008.05.010; (c) G. J. van der Vusse, Albumin as Fatty Acid Transporter. *Drug Metabolism and Pharmacokinetics* 2009, *24*. 300-307.
30. (a) M. Henriksson, E. Nordling, E. Melles, J. Shafqat, M. Stahlberg, K. Ekberg, B. Persson, T. Bergman, J. Wahren, J. Johansson, H. Jornvall, Separate functional features of proinsulin C-peptide. *Cellular and Molecular Life Sciences* 2005, *62*. 1772-1778, DOI: DOI 10.1007/s00018-005-5180-6; (b) A. Pramanik, K. Ekberg, Z. Zhong, J. Shafqat, M. Henriksson, O. Jansson, A. Tibell, M. Tally, J. Wahren, H. Jornvall, R. Rigler, J. Johnansson, C-peptide binding to human cell membranes: Importance of Glu27. *Biochemical and Biophysical Research Communications* 2001, *284*. 94-98, DOI: DOI 10.1006/bbrc.2001.4917.
31. T. Hach, T. Forst, T. Kunt, K. Ekberg, A. Pfutzner, J. Wahren, C-Peptide and Its C-Terminal Fragments Improve Erythrocyte Deformability in Type 1 Diabetes Patients. *Exp Diabetes Res* 2008. DOI: Artn 730594

Doi 10.1155/2008/730594.
32. S. Slinko, G. Piraino, P. W. Hake, J. R. Ledford, M. O'Connor, P. Lahni, P. D. Solan, H. R. Wong, B. Zingarelli, Combined Zinc Supplementation with Proinsulin C-Peptide Treatment Decreases the Inflammatory Response and Mortality in Murine Polymicrobial Sepsis. *Shock* 2014, *41*. 292-300, DOI: Doi 10.1097/Shk.0000000000000127.
33. (a) J. P. Richards, E. A. Bowles, W. R. Gordon, M. L. Ellsworth, A. H. Stephenson, R. S. Sprague, Mechanisms of C-Peptide-Mediated Rescue of Low O2-Induced Atp Release from Erythrocytes of Humans with Type 2 Diabetes. *American journal of physiology. Regulatory, integrative and comparative physiology* 2014. ajpregu 00420 2014, DOI: 10.1152/ajpregu.00420.2014; (b) J. P. Richards, G. L. Yosten, G. R. Kolar, C. W. Jones, A. H. Stephenson, M. L. Ellsworth, R. S. Sprague, Low O2-induced ATP release from erythrocytes of humans with type 2 diabetes is restored by physiological ratios of C-peptide and insulin. *American journal of physiology. Regulatory, integrative and comparative physiology* 2014, *307*. R862-8, DOI: 10.1152/ajpregu.00206.2014; (c) J. P. Richards, A. H. Stephenson, M. L. Ellsworth, R. S. Sprague, Synergistic effects of C-peptide and insulin on low O2-induced ATP release from human erythrocytes. *American journal of physiology. Regulatory, integrative and comparative physiology* 2013, *305*. R1331-6, DOI: 10.1152/ajpregu.00341.2013.
34. W. Medawala, P. McCahill, A. Giebink, J. Meyer, C. J. Ku, D. M. Spence, A Molecular Level Understanding of Zinc Activation of C-peptide and its Effects on Cellular Communication in the Bloodstream. *The review of diabetic studies : RDS* 2009, *6*. 148-58, DOI: 10.1900/RDS.2009.6.148.
35. C. P. Chen, Y. M. Wang, S. Y. Lockwood, D. M. Spence, 3D-printed fluidic devices enable quantitative evaluation of blood components in modified storage solutions for use in transfusion medicine. *Analyst* 2014, *139*. 3219-3226, DOI: Doi 10.1039/C3an02357e.

Fig.1

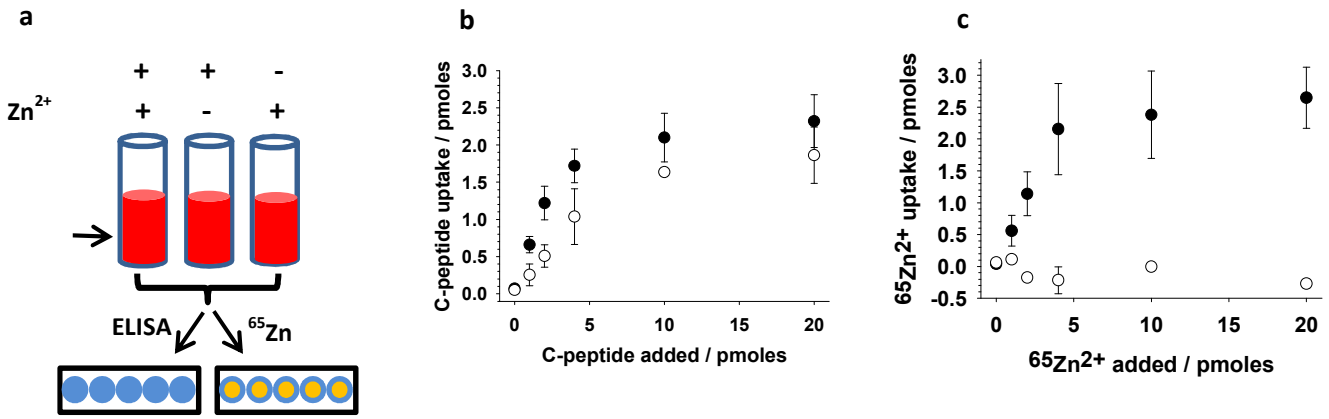

Fig.2

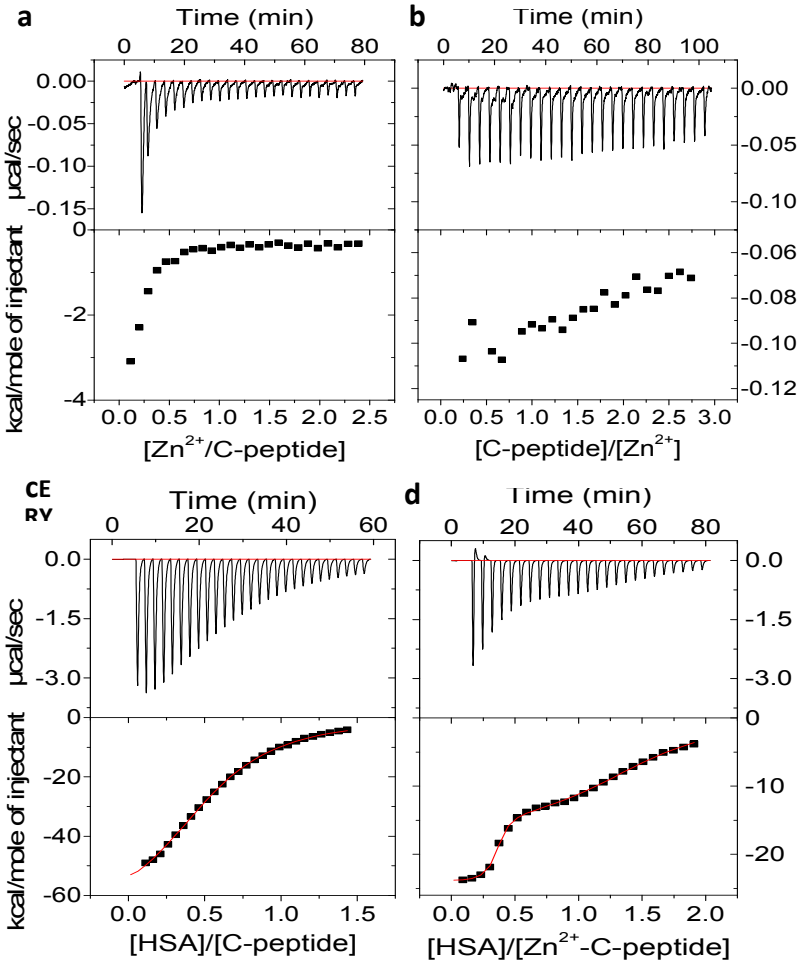

Fig.3

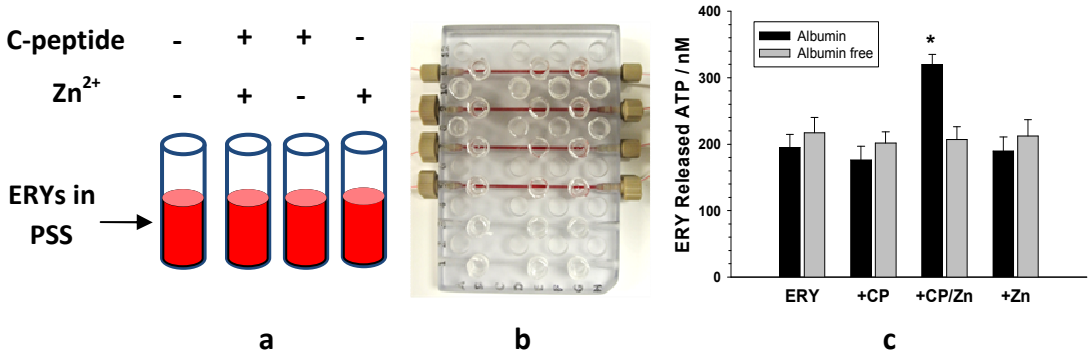

Fig.4

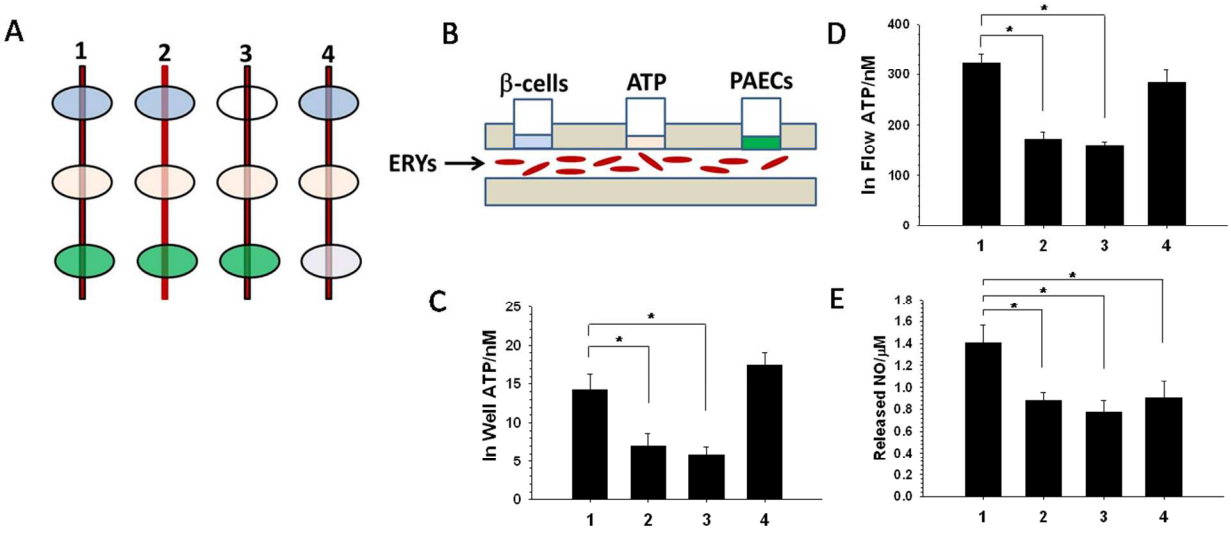

Figure Captions

Fig.1. C-peptide and Zn^{2+} binding to ERYs. The sample preparation strategy for C-peptide and $^{65}Zn^{2+}$ uptake by the ERYs is shown in **(a)**. A buffered PSS was incubated with equal molar concentrations of C-peptide, $^{65}Zn^{2+}$, or a combination of the two, resulting in final concentrations ranging from 0-20 nM for each, followed immediately by an appropriate aliquot of ERYs resulting in a 7% (v/v) solution of ERYs. After incubation for 2 hours at 37 °C, samples were centrifuged. The concentration of remaining C-peptide in the supernatant was measured by ELISA, and remaining $^{65+}Zn^{2+}$ was measured by scintillation counting. The C-peptide and $^{65}Zn^{2+}$ uptake was determined by subtracting the remaining moles in the supernatant from the original number of moles added to the ERY samples. The concentration-dependent C-peptide uptake by the ERYs in the presence (open circles) and absence (filled circles) of $^{65}Zn^{2+}$in albumin-containing PSS is shown in **(b)**. Saturable C-peptide uptake by the ERYs in the presence of $^{65}Zn^{2+}$ (2.0 picomoles) and absence of $^{65}Zn^{2+}$ (2.2 picomoles) was statistically equal (n=4, error bars are SEM, $p<0.05$). $^{65}Zn^{2+}$ uptake by the ERY in the presence (filled circles) and absence (open circles) of C-peptide in albumin-containing containing PSS is shown in **(c)**. $^{65}Zn^{2+}$ uptake by the ERYs in the presence of C-peptide saturated at approximately 2.5 pmoles, while no $^{65}Zn^{2+}$ uptake was by the ERY could be measured in the absence of C-peptide (n=3, error bars are SEM). These data suggest that C-peptide can bind the ERY in the presence and absence of Zn^{2+}, but Zn^{2+} binding to the ERY requires C-peptide.

Fig.2. Isothermal titration calorimetric (ITC) analysis of C-peptide, Zn^{2+}, and albumin binding. No specific binding between C-peptide and Zn^{2+} was observed when Zn^{2+} was titrated into C-peptide **(a)**, nor when C-peptide was titrated into Zn^{2+} **(b)**. Specific binding of HSA and C-peptide was observed in (**c)** ($N = 0.53 \pm 0.03$, averaged $K_a = 1.75 \pm 0.64 \times 10^5\ M^{-1}$, n=4). Specific binding of HSA to both C-peptide and Zn^{2+} is shown in (**d)** ($N_1 = 0.33 \pm 0.01$, $K_1 = 5.08 \pm 0.98 \times 10^7\ M^{-1}$; $N_2 = 1.15 \pm 0.01$, $K_2 = 2.66 \pm 0.25 \times 10^5\ M^{-1}$, n=3). A correction was applied for the heat of dilution.

Fig.3. The importance of albumin in C-peptide/Zn^{2+}-induced ATP release from ERYs. The sample preparation strategy for C-peptide/Zn^{2+} stimulation of ATP release from ERYs is shown in **(a)**. The protocol was similar to that describe in **Fig.1(a)** except that a non-radioisotopic version of Zn^{2+} was used and each sample was prepared in an albumin-containing and an albumin-free version of PSS. A 3D-printed fluidic device shown in **(b)** was used during the measurement of ERY-derived release of ATP. Four ERY samples were pumped into separate channels of the device and released ATP diffused from the channel through the porous membrane representing the bottom of the transwell insert (which had been manually loaded with 50 μL of PSS buffer just prior to ERY delivery to the device channels). The moles of ATP that diffused into the insert are proportional to the amount of ATP in the channel, enabling a quantitative determination of ERY-released ATP **(c).** While ATP was released from each ERY sample, a significant increase in ATP release was only measured from the ERY sample prepared in an albumin-containing buffer that had been incubated with both C-peptide and Zn^{2+}. The absence of any one of these 3 components (C-peptide, Zn^{2+}, or albumin) resulted in no significant increase in ERY-derived ATP (n=5, $p<0.005$).

Fig.4. Inter-tissue communication using a 3D-printed platform. Top-down, color-coded view of the strategies used to study inter-tissue communications between INS-1 cells, ERYs, and endothelial cells is shown in **(a)**. Each channel contained flowing ERY samples (red bars) and membrane inserts (colored ovals) above the channels for either INS-1 culture (top, blue ovals), ATP measurement (middle, orange ovals), or endothelial cell culture (bottom, green ovals). An actual image is shown in Fig. S2 in SI. Channel 2 did not contain any albumin in the flowing PSS buffer (lighter red flow channel), while channel

3 did not contain INS-1 cell (clear oval). Channel 4 contained endothelial cells incubated with PPADS to block ATP binding to the P2Y purinergic receptor on these cells. A schematic side view of the system is shown in **(b),** where secretions from the INS-1 cells (labeled as β-cells) can diffuse into the stream of ERYs; the resultant ATP release from the ERYs can be measured in the second insert well, while ATP-stimulated NO by the endothelial cells (bPAECs) is determined in the last insert. The amount of ERY-derived ATP that diffused into the middle inserts on each channel is shown in **(c).** Note the significant decrease when albumin is absent from the ERY stream (channel 2) or when there are no INS-1 cells (channel 3). The amount of ERY-derived ATP measured in the channel is shown in **(d)** and shows the same trend as in **(c)**, specifically, albumin and INS-1 cell secretions are required for increases in ERY-derived ATP. The concentration of NO production from endothelial cells **(e)** is greatest for channel 1, where albumin and INS-1 cells are present. Importantly, channel 4 NO production is also reduced due to the blocking of ATP binding to endothelial cells by PPADS. For all channels, n=5 ERY biological samples and error bars represent the SEM of those measurements, * represents values statistically different from channel 1, $p<0.01$.